

Tin–Tin Dioxide@Hollow Carbon Nanospheres Synthesized by Aerosol Catalytic Chemical Vapor Deposition for High-Density Lithium Storage

Jeong Hoon Byeon*^[a] and Young-Woo Kim*^[b]

The gas-phase self-assembly of Sn-SnO₂@hollow carbon nanospheres (HCNSs) synthesized by floating catalytic chemical vapor deposition, as a new, facile, and scalable method, was performed, and the resultant nanospheres displayed an enhanced lithium storage performance. Freshly synthesized Sn nanoparticles [≈ 25 nm in equivalent mobility diameter (EMD)] were incorporated quantitatively with dimethyl sulfide (DMS)-ethanol (EtOH) droplets (≈ 45 nm in EMD) in the form of Sn/DMS-EtOH hybrid droplets (≈ 42 nm in EMD). The hybrid droplets were employed to perform catalytic chemical vapor synthesis in a heated tubular reactor. It was observed that Sn-SnO₂ particles with sizes between 3–6 nm were dispersed in the HCNSs (≈ 25 nm in lateral dimension), and no bulky aggregates were visible. Its reversible capacity even increased up to ≈ 870 mA h g⁻¹ after 50 cycles, which is much higher than the conventional theoretical capacity of SnO₂ (782 mA h g⁻¹).

Nanostructured materials have received much attention because of their new electronic, optical, and catalytic properties.^[1,2] One category of such materials, Sn-C hybrid nanostructures, are ideal active materials for high energy and power density Li ion batteries (LIBs).^[3] Sn-based materials deserve special attention as they offer a promising alternative to graphite because of their high theoretical capacity (Sn: 990 mA h g⁻¹, SnO₂: 790 mA h g⁻¹, compared with 372 mA h g⁻¹ for graphite).^[4] However, it is a significant challenge to control the Sn particle size and the uniformity of Sn particle dispersion in the carbon matrix using current synthesis technology because of the low melting point of Sn and the tendency of particle growth, especially during high-temperature carbonization.^[5] Despite the urgent need of these kinds of hybrid nanostructures, there are few well-established facile and scalable methods to synthesize these advanced nanostructures. Usually, the multistep coating, currently used for this kind of nanostruc-

tured electrode, is time consuming and tedious, which hinders the scale-up of the process significantly.^[6,7]


The present work introduces a continuous gas-phase self-assembly of Sn-SnO₂@hollow carbon nanospheres (HCNSs) through a new floating catalytic chemical vapor deposition (CCVD)^[8] method for the enhancement of Li storage. HCNSs usually have a porous shell and a protected inner cavity, which endow them with wide potential applications in LIBs, fuel cells, energy storage, catalysis, and drug delivery.^[9] The successful key to this method is rooted in the deagglomerated Sn particles within precursor droplets, which allow the dispersion of ultrafine Sn particles in the carbon matrix. A catalytic formation of the carbon network is another factor that prevents Sn particles from growing bigger during the high-temperature process.

A spark discharge^[10] produced Sn nanoparticles, and the particle-laden flow passed over the Collison atomizer orifice in which they mix with the atomized dimethyl sulfide (DMS)-ethanol (EtOH) solution to form hybrid droplets. The use of plasma discharges for nanoscale materials synthesis is a field that is developing rapidly. In particular, nonthermal plasmas at atmospheric pressure are attractive because of several factors conducive to efficiency.^[11] The droplets then passed through a heated tube reactor to perform CCVD, which results in Sn-SnO₂@HCNSs. This CCVD method, as a new setup of aerosol-assisted CVD,^[12–14] uses DMS-EtOH droplets to transport the precursors into a heated reaction zone to react with Sn nanoparticles to form the desired hybrid nanostructures^[15] with the aid of inert carrier gases. The emergence of this CCVD can help to solve the availability and delivery problems of precursors in conventional CVD.^[16] The hybrid nanostructures were separated by mechanical filtration and they were employed as active materials for high-density Li storage. The storage performance of the nanostructures from DMS and toluene as carbon sources are systematically compared and discussed.

The total number concentration (TNC), geometric mean diameter (GMD), and geometric standard deviation (GSD) of the Sn particles, which were measured by using a scanning mobility particle sizer (SMPS, 3936, TSI, USA), were 2.72×10^6 particles cm⁻³, 24.7 nm, and 1.56, respectively (Figure S1). Sn/DMS-EtOH hybrid droplets were formed by incorporating Sn with DMS-EtOH during the Collison atomization. We verified the incorporation of the Sn nanoparticles with the DMS-EtOH droplets by measuring the size distributions of DMS-EtOH and Sn/DMS-EtOH in the gas phase. The size distribution measurements of DMS-EtOH and Sn/DMS-EtOH are summarized in Table S1. The TNC, GMD, and GSD of the Sn/DMS-EtOH hybrid

[a] Dr. J. H. Byeon
Department of Chemistry
Purdue University
Indiana 47907 (USA)
E-mail: jbyeon@purdue.edu

[b] Dr. Y.-W. Kim
Department of Automotive Engineering
Hoseo University
Asan 336-795 (South Korea)
E-mail: ywkim@hoseo.edu

 Supporting information for this article is available on the WWW under <http://dx.doi.org/10.1002/cctc.201402013>.

droplets are 4.30×10^6 particles cm^{-3} , 41.9 nm, and 1.54, respectively. The analogous data for DMS-EtOH are 4.57×10^6 particles cm^{-3} , 44.5 nm, and 1.54, respectively. The size distribution of the Sn/DMS-EtOH droplets was more similar to that of the DMS-EtOH droplets than that of the Sn particles, and there was no characteristic bimodal distribution, which implies that the Sn particles were incorporated nearly quantitatively with DMS-EtOH to form Sn/DMS-EtOH hybrid droplets. The unimodal size distributions (2.74×10^6 particles cm^{-3} TNC, 26.1 nm GMD, and 1.54 GSD) of the Sn/DMS-EtOH remained constant even after CVD, however, the distribution shifted to a smaller size probably because of solvent (mostly EtOH) extraction during CVD, which indicates that the carbon precipitate consisted of solid structures.

TEM (JEM-3010, JEOL, Japan) images show the morphology of Sn, DMS-EtOH, and Sn/DMS-EtOH before and after CVD (Figure 1). Specimens were prepared for examination by TEM by direct electrostatic gas-phase sampling at a sampling flow of 1.0 L min^{-1} and an operating voltage of 5 kV by using a Nano Particle Collector (NPC-10, HCT, Korea). The TEM image reveals that the Sn particles were agglomerates (≈ 23 nm in the lateral dimension) of several primary particles (each ≈ 3.4 nm in the lateral dimension), which is consistent with the SMPS data (measured agglomerated Sn particles) noted in Table S1. Most Sn particles were encapsulated in the DMS-EtOH droplets if they passed over the orifice of the Collision atomizer, which resulted in Sn/DMS-EtOH hybrid droplets. The Sn particles were redistributed in the DMS-EtOH droplets as a result of deagglomeration (by setting the force acting on an agglomer-

ate of size D_{pa} because of the sudden pressure change across an orifice in the Collision atomizer), and the size is given by Equation (1):^[17]

$$D_{\text{pr}} = \alpha \sqrt{\frac{D_{\text{pa}} H}{6\pi \Delta P \Theta^2}} \quad (1)$$

in which D_{pr} is the size of a restructured agglomerate, α is the proportionality constant, H is the Hamaker constant, ΔP is the pressure difference between the front and the rear of the orifice, and Θ is the parameter that controls the maximum cohesive strength between the constituent particles in an agglomerate. Sn agglomerates pass through the orifice, and the rapid changes in pressure, density, and velocity across the orifice produce an impulse able to shatter the agglomerates. Therefore, this floating CCVD may be a suitable strategy to synthesize Sn-SnO₂@HCNSs with Sn particles dispersed uniformly in the carbon matrix. A TEM image shows the nanostructures after CVD, which shows the conservation of the spherical geometry and outer diameter of ≈ 25 nm. All the nanostructures had a hollow cavity and the morphology was fairly uniform. The lighter color in the structures represents the carbon fringes, and the darker color represents the metallic Sn particles. The high-resolution TEM images reveal that the Sn particles in the carbon layers (≈ 5 nm in thickness) are around 4 nm. The interlayer distance between the graphene planes was ≈ 0.352 nm, which is larger than that of normal graphite (≈ 0.335 nm). This is an indication that the crystallinity of the

carbon in the nanostructures is yet to match that in graphite. The Sn-SnO₂ particles exhibited a lattice fringe spacing of 0.29 nm (Figure 1), which could be indexed as the (200) plane of the tetragonal Sn structure. Another TEM image shows that lattice fringes exist with a d spacing value of 0.27 nm, which corresponds to the (101) plane of SnO₂ and suggests the existence of SnO₂ particles in the HCNSs. The C, Sn, and O mass ratio of the HCNSs was 0.66:0.25:0.09, which was measured by energy dispersive X-ray spectroscopy (JED-2200, JEOL, Japan). As a result of the use of EtOH as the precursor solvent, hydrolysis occurred, which was the primary reaction that resulted in the formation of SnO₂ particles. Nevertheless, one could envisage that the close contact between the Sn-SnO₂ particles and carbon layers allowed good electron-transfer pathways.

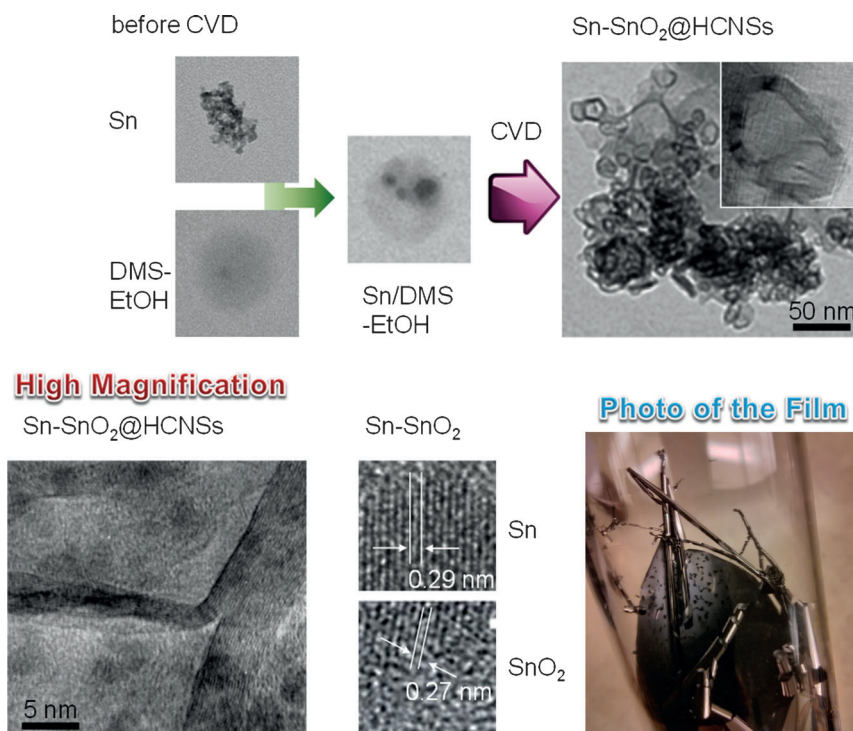


Figure 1. TEM images of spark-produced Sn (23 ± 4.9 nm), Collision-atomized DMS-EtOH (48 ± 2.6 nm), and Sn/DMS-EtOH (40 ± 1.4 nm) samples before CVD. Low- and high-magnification TEM images of Sn-SnO₂@hollow carbon nanosphere hybrid materials (25 ± 6.1 nm) with their film (photo) are also displayed.

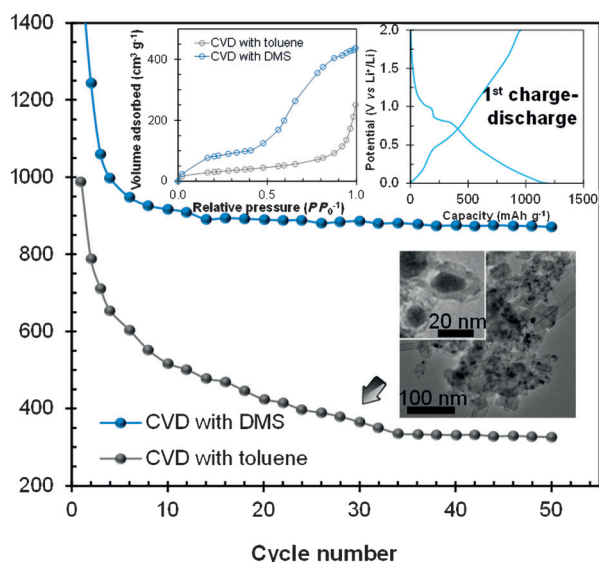


Figure 2. Cyclic Li storage performances for Sn/DMS-EtOH and Sn/toluene-EtOH samples after CVD. Adsorption isotherms of both samples are also shown (inset). Low- and high-magnification TEM images for Sn/toluene-EtOH after CVD are also depicted (inset).

In the first cycle (inset in Figure 2), the HCNSs electrode exhibited a Li-insertion capacity of 1163 mAh g^{-1} . Despite a decrease in the initial stage, the charge capacity of Sn-SnO₂@HCNSs was maintained after 50 cycles and remained at 74.8% (870 mAh g^{-1}) of the initial value, which highlights the synergetic effect for enhanced cyclic performance. The cyclic performances of samples from Sn/DMS-EtOH and Sn/toluene-EtOH hybrid droplets are shown in Figure 2. Large Sn-SnO₂ particles (TEM image in Figure 2) encapsulated fully in the hollow carbon structures exhibited rapid capacity fading within 30 cycles, which shows a charge capacity below 350 mAh g^{-1} . Compared to Sn/toluene-EtOH (the size distribution and Raman spectrum of which are shown in the Supporting Information), the reversibility of Sn/DMS-EtOH was enhanced significantly, which reveals the influence of a hollow carbon matrix with Sn and SnO₂ particles. Although many factors may contribute to those differences, the main reason for the poor cycle life of Sn/toluene-EtOH may be caused by a smaller pore volume to buffer the huge volume expansion produced by the alloying reaction between Li and Sn,^[18] which leads to the pulverization and subsequent electrical disconnection of the electrodes. N₂ adsorption measurements (Micromeritics ASAP 2010) with the BET method were used to determine the porosity of the hybrid nanostructures and to check the possibility of interconnected pores in the structures (inset of Figure 2). The overall shapes of the adsorption isotherms indicate their meso- and macroporous characteristics. The uptakes at >0.85 and <0.85 P/P_0 may originate from the void spaces among agglomerated HCNSs and the hollow cores of HCNSs, respectively.^[9] The product from Sn/DMS-EtOH has a higher BET surface area ($672 \text{ m}^2 \text{ g}^{-1}$) and larger pore volume ($0.61 \text{ cm}^3 \text{ g}^{-1}$) than that ($354 \text{ m}^2 \text{ g}^{-1}$ and $0.20 \text{ cm}^3 \text{ g}^{-1}$) from Sn/toluene-EtOH. The pores within Sn/DMS-EtOH could show a better structure as buffering spaces against the volume change of Sn and SnO₂

particles upon the charge-discharge process and help with ion transport, which eventually lead to enhanced cyclic performances in an LIB. This tendency was also consistent in other Li storage tests with sintered (at 500°C , Figure S2) nanostructures. This implies that the materials with a hollow structure and large surface area may be flexible even at high temperatures to display higher reversible capacities as Li ions stored in the interfaces and pores of the material could take part in the reaction.

We developed for the first time a new floating catalytic CVD method to synthesize Sn-SnO₂@HCNSs for efficient Li storage. Compared with Sn/toluene-EtOH, there were larger pore volumes inside the hollow carbon matrix and the ultrafine Sn-SnO₂ particles were dispersed in the carbon matrix. The synthesized nanostructures not only utilized the ultrafine Sn particles to store Li ions, which thus provides high capacity, but also improved the cycling stability. The superior cycling performance was also attributed to the sizes of the Sn-SnO₂ particles. A reduced size could reduce the strain and improve the electrochemical properties of the electrode materials significantly. Furthermore, the hollow carbon frame that contains S atoms, which acts to release the strain, could accommodate the large volume change and prevent Sn aggregation over repeated cycling. The proposed method opens up a new way to obtain hybrid carbonaceous nanostructures for a broad range of practical applications.

Keywords: carbon • chemical vapor deposition • nanostructures • self-assembly • tin

- [1] C.-H. Lai, M.-Y. Lu, L.-J. Chen, *J. Mater. Chem.* **2012**, 22, 19.
- [2] J. Sun, H. Liu, X. Chen, D. G. Evans, W. Yang, X. Duan, *Adv. Mater.* **2013**, 25, 1125.
- [3] F. Han, W.-C. Li, M.-R. Li, A.-H. Lu, *J. Mater. Chem.* **2012**, 22, 9645.
- [4] G. Cui, Y.-S. Hu, L. Zhi, D. Wu, I. Lieberwirth, J. Maier, K. Müllen, *Small* **2007**, 3, 2066.
- [5] Y. Xu, Q. Liu, Y. Zhu, Y. Liu, A. Langrock, M. R. Zachariah, C. Wang, *Nano Lett.* **2013**, 13, 470.
- [6] Y. Qiu, K. Yan, S. Yang, *Chem. Commun.* **2010**, 46, 8359.
- [7] J. Liu, Y. Zhou, C. Liu, J. Wang, Y. Pan, D. Xue, *CrystEngComm* **2012**, 14, 2669.
- [8] M. J. Kim, S. Chatterjee, S. M. Kim, E. A. Stach, M. G. Bradley, M. J. Pender, L. G. Sneddon, B. Maruyama, *Nano Lett.* **2008**, 8, 3298.
- [9] R. Jia, J. Chen, J. Zhao, J. Zheng, C. Song, L. Li, Z. Zhu, *J. Mater. Chem.* **2010**, 20, 10829.
- [10] J. H. Byeon, J.-W. Kim, *Appl. Phys. Lett.* **2010**, 96, 153102.
- [11] D. Z. Pai, K. Ostrikov, S. Kumar, D. A. Lacoste, I. Levchenko, C. O. Laux, *Sci. Rep.* **2013**, 3, 1221.
- [12] X. Hou, K.-L. Choy, *Chem. Vap. Deposition* **2006**, 12, 583.
- [13] Y. Tian, M. Y. Timmermans, M. Partanen, A. G. Nasibulin, H. Jiang, Z. Zhu, E. I. Kauppinen, *Carbon* **2011**, 49, 4636.
- [14] C. Castro, M. Pinault, S. Coste-Leconte, D. Porterat, N. Bendjab, C. Reynaud, M. Mayne-L'Hermite, *Carbon* **2010**, 48, 3807.
- [15] W.-H. Chiang, R. M. Sankaran, *Appl. Phys. Lett.* **2007**, 91, 121503.
- [16] W. Ren, F. Li, S. Bai, H.-M. Cheng, *J. Nanosci. Nanotechnol.* **2006**, 6, 1339.
- [17] J. H. Byeon, J. T. Roberts, *ACS Appl. Mater. Interfaces* **2012**, 4, 2693.
- [18] Y. Kwon, H. Kim, S.-G. Doo, J. Cho, *Chem. Mater.* **2007**, 19, 982.

Received: February 5, 2014

Revised: February 24, 2014

Published online on April 9, 2014